Check for updates Green Chemistry



Cutting-edge research for a greener sustainable future

Accepted Manuscript

This article can be cited before page numbers have been issued, to do this please use: E. F. Fiandra, M. starck, E. K. Findlay, J. Binks, G. Si, R. Chilton, M. R. Sivik, R. Thompson, M. R. Wilson and C. Mahon, Green Chem., 2025, DOI: 10.1039/D5GC04056F.



This is an Accepted Manuscript, which has been through the Royal Society of Chemistry peer review process and has been accepted for publication.

Accepted Manuscripts are published online shortly after acceptance, before technical editing, formatting and proof reading. Using this free service, authors can make their results available to the community, in citable form, before we publish the edited article. We will replace this Accepted Manuscript with the edited and formatted Advance Article as soon as it is available.

You can find more information about Accepted Manuscripts in the Information for Authors.

Please note that technical editing may introduce minor changes to the text and/or graphics, which may alter content. The journal's standard Terms & Conditions and the Ethical guidelines still apply. In no event shall the Royal Society of Chemistry be held responsible for any errors or omissions in this Accepted Manuscript or any consequences arising from the use of any information it contains.



View Article Online

DOI: 10.1039/D5GC04056F

Green foundation

1) Soil release polymers (SRPs) are used in laundry detergent formulations to enable effective cleaning performance during shorter cycles at low wash temperatures, presenting clear environmental benefits. Most SRPs are constructed using petroleum-derived building blocks, limiting their environmental benefits. Here, we report a new class of SRPs where a proportion of a petroleum-derived monomer, terephthalic acid, is replaced with a biomass-derived alternative, diglyoxylic acid xylose.

- 2) SRPs are shown to match the performance of conventional SRPs on polyester substrates and to exceed performance of currently used SRPs on polyspandex. These SRPs therefore present enhanced cleaning performance and improved environmental profile.
- 3) Our studies have provided insights into the mechanism of surface modification by SRPs, which will guide the future design of biobased detergent additives.

View Article Online DOI: 10.1039/D5GC04056F

ARTICLE

Polyesters incorporating biobased monomers for soil-release treatment of synthetic textile surfaces

Received 00th January 20xx. Accepted 00th January 20xx

DOI: 10.1039/x0xx00000x

Emanuella F. Fiandra, Matthieu Starck, Elliot K. Findlay, Josephine Binks, Gang Si, Ruth Chilton, Mark R. Sivik, Richard L. Thompson, Mark R. Wilson, Clare S. Mahon

Soil release polymers (SRPs) are used in laundry detergent formulations to enable the cleaning of textiles at lower wash temperatures and using shorter cycles. By modifying the fabric surface, SRPs prevent redeposition of soil during the wash cycle, and also assist with the removal of soil in the subsequent wash cycle. Most SRPs currently used in formulations contain petroleum-sourced building blocks, including terephthalic acid, potentially limiting the environmental benefit of their use. To improve the sustainability profile of these key additives, diglyoxylic acid xylose (DGAX, 1), a monomer derived from hemicellulose, was used to partially replace the terephthalic acid component of SRPs. The ability of these copolymers to modify fabric surfaces was explored using anti-redeposition and soil release performance tests, in addition to contact angle and SEM analysis. The introduction of 1 within copolymers was found to further enhance the anti-redeposition performance on polyspandex fabrics, however, complete replacement of the terephthalic acid component with 1 resulted in polymers which displayed poor performance. These copolymer systems present a promising route to the development of highperformance and sustainable SRPs, particularly in offering performance across different synthetic textile surfaces.

Introduction

Synthetic polyester fibres were first introduced in the 1960s as a more durable and cheaper alternative to cotton and wool garments.1 Synthetic fabrics can offer a more sustainable environmental footprint, as cotton is a highly water-intensive fabric during production and in fabric care and maintenance,2 accounting for 69% of the water footprint for fibre production alone.3,4 Polyester (typically poly(ethylene terephthalate), PET, Figure 1) fabrics are low-cost, durable, easy-to-wash and wrinkle-free, with an annual production of 57 million tonnes in 2020, representing 52% of global fibre production.⁵ Compared to cotton, synthetic fibres such as PET and polyspandex (PS, Figure 1), a blend of polyethylene terephthalate and a polyurethane, are more regular in structure and hydrophobic in nature, which can lead to challenges in the removal of hydrophobic soil^{6, 7} such as grease, sebum, or cooking oil. The build-up of such soil on synthetic fabrics can lead to issues with

the appearance⁸ or odour^{9, 10} of fabrics, and loss of moisture comfort.11 Within modern detergent formulations, polymer additives12-17 are used to circumvent these challenges in soilremoval and to prevent transfer of dyes between fabrics, with improvements in cleaning performance sufficient to enable efficient cleaning under milder wash settings of 30 °C, rather than 40 °C, facilitating energy reductions of up to 40% per cycle.18

Soil release polymers (SRPs) deposit on fibres, and hence change the surface properties, 19, 20 delivering benefits such as reducing soil deposition onto the fabric during the wash cycle and further promoting the removal of soil from SRP-modified fabric surfaces in the next wash cycle (Figure 1). SRPs also reduce the adhesion of allergens to the fabric, 21, 22 reduce malodour on consumer garments,23-27 and improve wicking properties.^{28, 29} These improvements in fabric appearance and comfort can also extend the service life of textiles, offering further sustainability benefits, with extended garment lifetimes contributing to reductions in the amounts of textile waste disposed of in landfill sites.4 The presence of aromatic units in conventional SRPs is critical for their deposition, with these units predominantly derived from terephthalate monomers (Figure 1a), which are obtained through the oxidation of petrochemically sourced p-xylene.30 While advances have been made in the production of terephthalic acid from biomass,31-33

^{a.} Department of Chemistry, Durham University, Durham, DH1 3LE, UK

b. The Procter & Gamble Newcastle Innovation Centre, Whitley Rd, Newcastle upon Tyne, NE12 9BZ, UK.

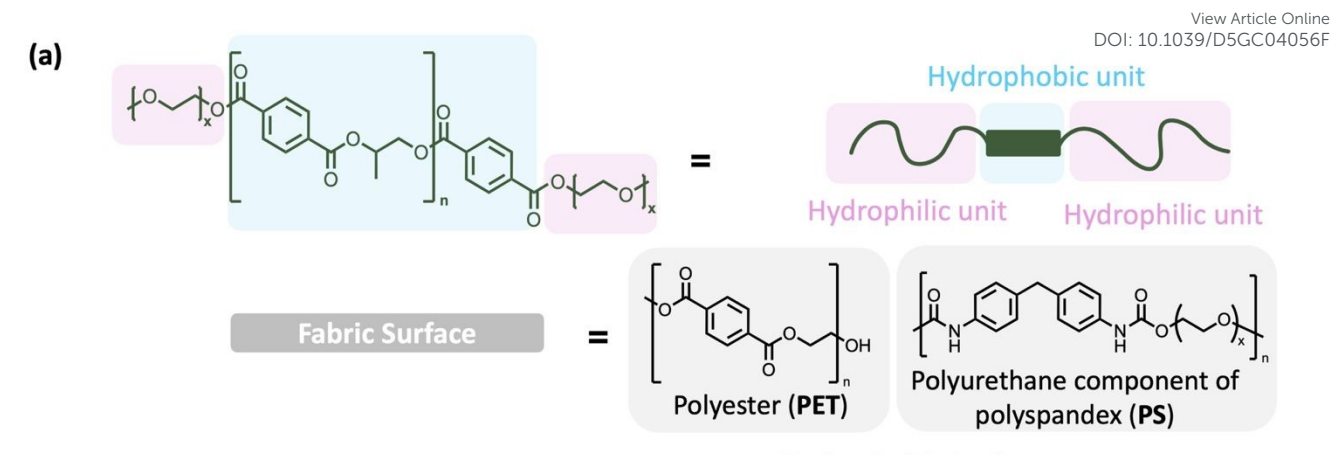
^c Fabric & Home Care Innovation Center, The Procter & Gamble Company, Cincinnati. Ohio 45202. USA

[†] Footnotes relating to the title and/or authors should appear here. Supplementary Information available: [synthetic methods, characterisation, performance testing, computational methods]. See DOI: 10.1039/x0xx00000x

This article is licensed under a Creative Commons Attribution 3.0 Unported Licence.

Open Access Article. Published on 15 octombrie 2025. Downloaded on 17.10.2025 14:13:21.

ARTICLE Journal Name



Hydrophobic Surface

(b) 35

View Article Online DOI: 10.1039/D5GC04056F

ARTICLE

Figure 1: (a) A conventional terephthalate-based SRP, with the hydrophilic and hydrophobic components highlighted and the hydrophobic fabric surfaces of interest: polyester (PET); and the polyurethane component of polyspandex (PS). (b) The proposed mechanism of SRP function. SRPs deposit on fabric surfaces, rendering the surface hydrophilic and hence preventing staining during the next wear phase, with multi-cycle enhancement during subsequent wash cycles.

approaches are currently less efficient than traditional petrochemical routes. More generally, the need to move away from petrochemically-derived feedstocks has resulted in rising interest in sustainably sourced monomers³⁴ and monomers that are biobased,³⁵ to improve the sustainability profile of these key detergent additives.36-39

One attractive alternative to petrochemical-based feedstocks is the use of lignocellulosic biomass, due to the inherently degradable nature and high abundance of these materials. 40-43 Lignocellulose is comprised of three principal fractions: cellulose, hemicellulose and lignin; organised into macrofibrils which mediate the structural stability of plant cell walls.44 Hemicellulose is the second most abundant component in lignocellulose, and when hydrolysed gives rise to the 5- and 6- carbon monosaccharides glucose, xylose, arabinose, galactose and mannose.⁴⁵ For low-cost production of sugars,⁴⁶ sources high in hemicellulose and low in lignin content such as birch wood⁴⁷ and corn cobbs⁴⁸ provide a promising supply. Manker et al reported⁴⁹ the synthesis of biosourced polymers derived from monomers prepared from the hemicellulosic fraction extracted from birch wood in a high yielding, scalable process. In this approach, the fused heterotricyclic diacid diglyoxylic acid xylose (DGAX) (1), and the corresponding dimethyl ester, dimethylglyoxylate xylose, were produced though the reaction of xylose with diglyoxylic acid, and used to

make polyesters. It was additionally shown that these monomers can be accessed directly from hemicellulose via aldehyde-assisted fractionation⁵⁰ to produce xylose, which can then be transformed into the diacid monomers. Similar approaches have also been used to synthesise biobased surfactants from lignocellulosic biomass. 51-53 Lignocellulose and derivatives have been used⁵⁴ to permanently modify fabric surfaces to infer functionality such as UV resistance and fire retardancy, demonstrating the potential of these biomass derived materials to modify surface properties.

In this paper, we report the synthesis of a series of SRPs (P1-P5) that contain varying proportions of biobased monomer 1 and dimethyl terephthalate (2) and explore their performance in laundry detergent formulations. To gain further insight into the differences in wash performance and establish structureproperty relationships, the behaviour of SRPs in solution and at the textile interface was studied in simplified systems using a range of techniques: contact angle measurements, scanning electron microscopy (SEM) and dynamic light scattering (DLS).

Scheme 1: Synthesis of SRPs P1-P5 using melt polycondensation approach.

Table 1: Synthesis and resultant structural parameters of SRPs. (eq.: molar equivalent)

a As determined by 1H NMR spectroscopy, using end-group -OCH3 as reference for analysis. B As determined by gel permeation chromatography in 1.0 g/LiBr in DMF at 50 °C (0.6 mL min⁻¹), calibrated against near monodisperse poly(methyl methacrylate) standards.

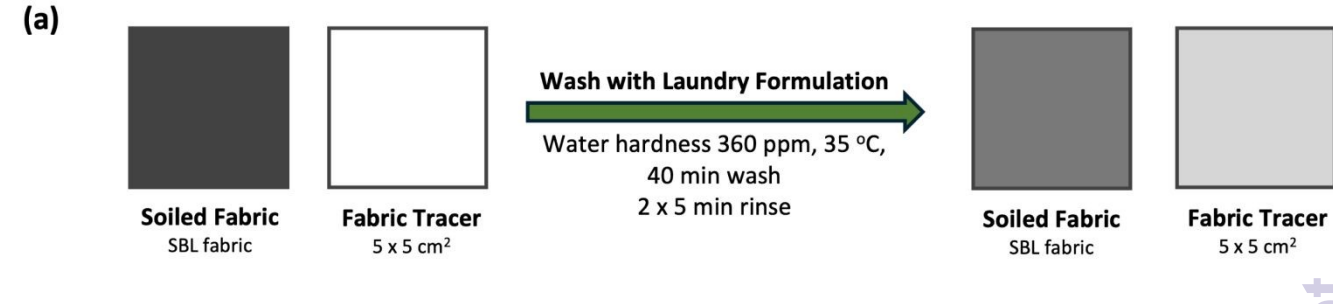
Molecular modelling was used to compare binding affinities for SRP cores to representative PET and PS surfaces, and provide insights into the folding and aggregation of SRPs in water. We demonstrate that incorporation of 1 into SRPs leads to strong

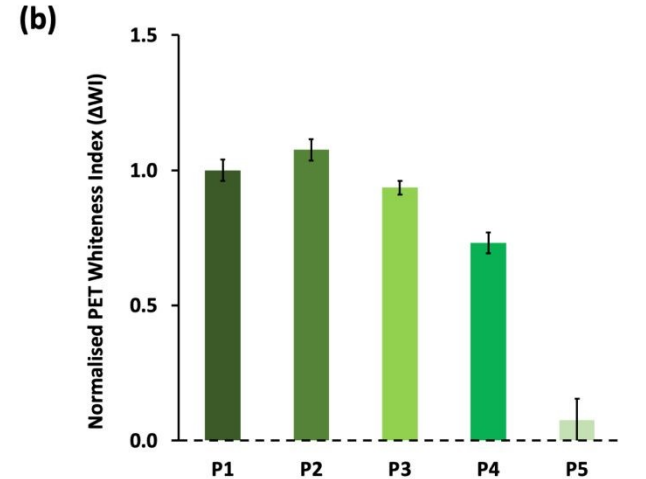
binding to both fabrics, significantly increasing binding affinity for PS. However, strong intra-chain interactions between units of 1 increase solution aggregation such that SRPs containing larger proportions of 1 form larger aggregates (surrounded by a

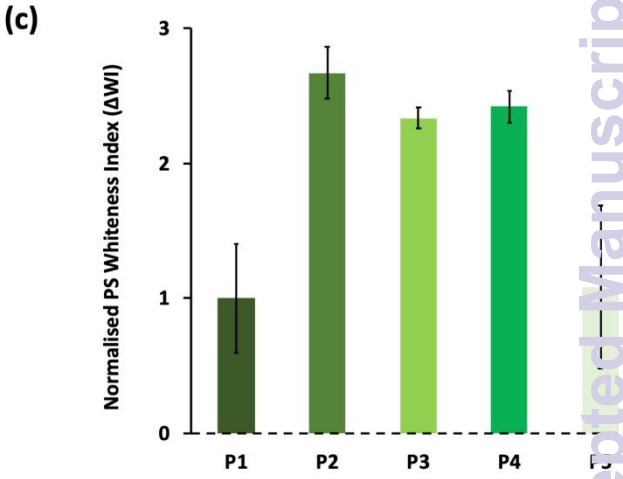
Polymer	1 / eq.	2 / eq.	3 / eq.	4 / eq.	nª	mª	DP	% of 1	$M_{ m n}^{ m a}/$ g mol ⁻¹	<i>M</i> _n b/ g mol⁻¹	M _w b / g mol⁻¹	Ð♭
P1	0.0	10	400	2.0	5	0	5	0	5200	5800	6400	1.1
P2	1.0	9.0	400	2.0	6	1	7	12	5600	6000	6600	1.1
Р3	2.0	8.0	400	2.0	6	2	8	25	6000	6200	6800	1.1
P4	5.0	5.0	400	2.0	3	3	6	50	5600	5200	5900	1.1
P5	20	0.0	400	2.0	0	6	6	100	6000	5700	6200	1.1

ARTICLE Journal Name

PEG corona) that do not adhere effectively to fabric surfaces. Combining 1 and 2 in the central block of the polymer disrupts







solution aggregation, yielding SRPs that match the performance of currently used SRPs on PET, and show a markedly improved performance on PS fabrics.

were attained across the series P1-P5 (Table 1; ESI Figure S1).

Results and discussion

Polymer synthesis and characterisation

series of poly(propylene terephthalate) (P1) and poly(propylene diglyoxylic acid xylose) (P5) based SRPs, and their corresponding copolymers (P2-P4) were prepared under classical melt polycondensation conditions (Table 1), following a protocol adapted from the literature.⁴⁹ Classical melt polycondensation typically requires highly temperatures due to the requirement for a polycondensation to be at least 10 to 20 °C higher than the melting point of both monomers and polymers to achieve melt homogeneity.55 Pentaerythritol tetrakis[3-[3,5-di-tert-butyl-4hydroxyphenyl] propionate (Irganox1010) was therefore added to reaction mixtures to avoid thermo-oxidative degradation of monomers.

Following this method, a series of homopolymers and copolymers were prepared using 1/2 as the dicarboxylate component (Table 1). The stoichiometric ratio of 1 and 2 was varied to produce polymers containing 0-100% 1 as the dicarboxylate component. The resultant polymers were analysed by ¹H NMR spectroscopy (ESI Section 8.2) and gel permeation chromatography (GPC) (ESI Section 2.5) to confirm the structure of the polymer, and determine the degree of

Anti-Redeposition Performance

The ability of **P1-P5** to function in laundry detergent formulations was initially investigated using anti-redeposition performance tests. Here, SRPs are evaluated for their ability to prevent the redeposition of suspended soil, transferred from a soiled fabric swatch, onto white fabric tracers during the wash process (Figure 2a). The extent of soil redeposition is monitored by assessing the whiteness index (WI) of the fabric tracers before and after washing under standard D65 illumination by image analysis (ESI Section 3.1).

A high-throughput tergotometer system was used to evaluate the anti-redeposition performance of **P1-P5**, with PET and PS tracers washed under representative wash conditions (40 min wash, 2×15 min rinse, 35 °C, water hardness 360 ppm, 4 cycles). Each wash load also included knitted cotton and polycotton fabric swatches to represent a consumer wash load, along with soil. Commercially-sourced artificial soil sheet (SBL2004 WFK, Krefeld, Germany) were cut into 5×5 cm² squares and included in each wash together with white PE and PS fabric tracers (also 5×5 cm² squares) with the soil consisting of vegetable oil, synthetic sebum and solid particles such as carbon black and kaolin. Soiled fabric sheets were replaced after each wash cycle, and image analysis was used to quantify anti-redeposition performance in terms of the change in

Sreen Chemistry Accepted Manuscr

View Article Online DOI: 10.1039/D5GC04056F

ARTICLE

Figure 2: (a) Anti-redeposition performance test under standard wash conditions; (b) Normalised whiteness index (ΔWI) of polyseter (PET) tracers and (c) normalised whiteness index (ΔWI) of polyspandex (PS) tracers washed with a laundry detergent formulated with 1% (w/w) SRP (P1-P5), with data normalised relative to P5. The baseline 0 indicates the performance of the polymeric additive-free negative control (Nil).

whiteness index (Δ WI) of PET or PS tracers. A negative control experiment (Nil) was performed, with no SRPs present in the detergent formulation, to allow for a direct comparison with detergent formulation containing SRPs under study (1% w/w). The Δ WI was determined by comparing the WI of fabric tracers washed with SRP-containing formulations to the WI of the negative control. SRPs that perform well produce a high positive Δ WI value.

P1, which is representative of conventional terephthalatebased SRPs, showed a significant whiteness benefit for PET fabrics (Figure 2b), as expected due to its similarity in structure to the surface enabling favourable supramolecular interactions between the core block of the SRP and the PET surface.56 Interestingly, copolymers P2-P4 exhibited similar performance on PET, comparable to that of the homopolymer P1. Conversely, P5 demonstrated little to no performance on PET fabric, demonstrating inclusion of a proportion of monomer 2 to be crucial to anti-redeposition performance. Results for P2 and P3, however. suggest that equivalent anti-redeposition performance on PET fabrics can be achieved at dicarboxylate monomer compositions of up to 25% bioderived monomer 1.

Interestingly, the anti-redeposition performance benefit of SRPs containing both dicarboxylate components (**P2-P4**) on PS fabric was greater than that of either **P1** or **P5**, with average Δ WI at least doubling in value (Figure 2c). SRPs currently used in formulations typically display limited anti-redeposition performance on PS fabrics, analogous to observations for **P1**. PS fabrics are typically comprised of a blend of both PET and polyether-polyurea fibres, most commonly 95% PET and 5% polyether-polyurea. The inclusion of **1** therefore offers a marked benefit to SRP performance in extending anti-redeposition performance to PS fabrics, enabling effective cleaning of PS fabrics under environmentally favourable conditions.

Soil Release Performance

P1-P5 were subsequently evaluated in soil release performance tests to further investigate the surface modification capabilities of the SRPs. PET and PS tracers $(5 \times 5 \text{ cm}^2)$ were preconditioned with a laundry detergent formulation containing 1% w/w SRP in a high-through put tergotometer system, mimicking typical consumer wash conditions (final SRP concentration 20 ppm, 40

min wash, 2 × 15 min rinse, 30 °C, water hardness 135 ppm, 3 cycles) (Figure 3a). Each wash load included eight tracers and knitted cotton swatches to represent a consumer wash load. Once dried (50% relative humidity, 20 ± 2 °C), each fabric tracer was stained with 100 μ L dirty motor oil (DMO) (ESI, Section 3.2) and left to dry overnight. Stained PET and PS tracers then underwent image analysis before washing under standard wash conditions (40 min wash, 2 × 15 min rinse, 30 °C, water hardness 135 ppm, 1 cycle), with the laundry detergent formulation used

This article is licensed under a Creative Commons Attribution 3.0 Unported Licence.

Open Access Article. Published on 15 octombrie 2025. Downloaded on 17.10.2025 14:13:21

ARTICLE Journal Name

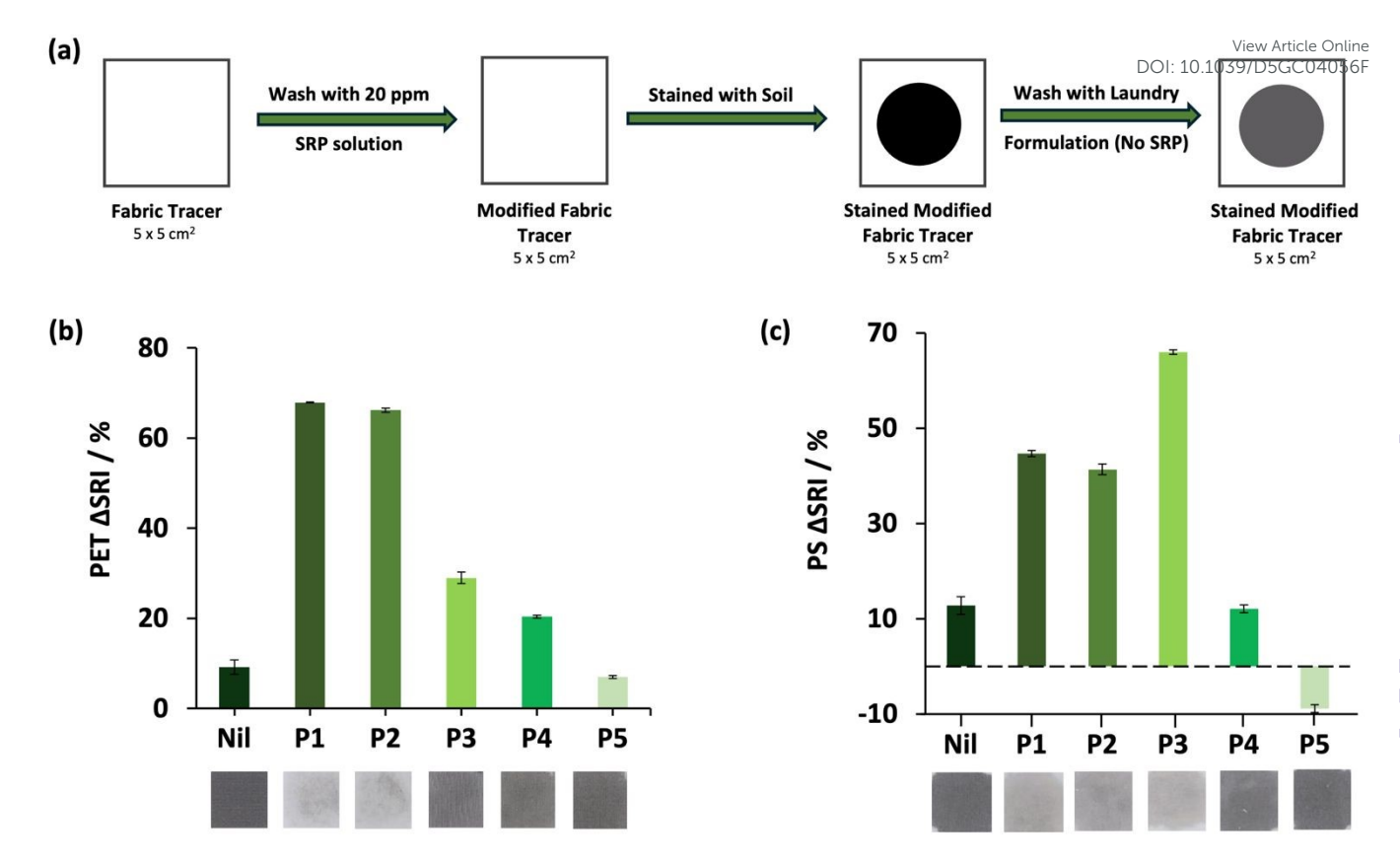


Figure 3: (a) Soil release performance test conducted under standard wash conditions; (b) \(\Delta SRI \) values obtained for the Nil and SRPs P1 to P5 on PET tracers; (c) \(\Delta SRI \) values obtained for the Nil and SRPs P1 to P5 on PS tracers with photographs of the fabric tracers after performance testing.

containing no SRPs. During the final wash stage, each load included two tracers of either PET or PS and knitted cotton garments. Four replicates were run in total for each polymer sample under investigation. Once dried, images were collectedfor each of the tracers, with the pre- and post-wash data analysed. Here, the colour of the fabric surface was characterised by measuring the L* (lightness), a* (redness), and b* (blueness) coordinates, as defined by the CIELAB colour system. The relative colour changes, ΔE^* , were then determined from the differences in these coordinates before and after the final wash cycle, which were then used to calculate the stain removal index (SRI) (ESI, Section 3.2). Betterperforming SRPs remove DMO from fabrics more effectively, represented by a higher SRI (%).

PET surfaces modified with **P2** resulted in an Δ SRI value of 66.2 \pm 0.6% which was comparable to the conventional polymer **P1** (67.9 \pm 0.1%) (Figure 3b). This observation suggests that the incorporation of 12% of monomer **1** into the central block of the SRP does not negatively impact the soil release performance. **P3** and **P4**, however, displayed a significantly lower performance with Δ SRI values ranging from 20 to 29%. **P5** displayed the lowest Δ SRI value of 9 \pm 2%, highlighting its inability to effectively facilitate the removal of DMO from a treated surface during a wash cycle. A different trend is observed when PS surfaces are treated with polymers containing **1** (Figure 3c), with the copolymer **P3** displaying high Δ SRI value of 66 \pm 1%, respectively, exceeding that of the conventional polymer **P1** (45

 \pm 1%). **P4** and **P5** displayed marked decreases in performance, however. In gravimetric sebum removal tests (ESI Section 3.3) **P2-P4** were observed to display comparable performance to the conventional SRP, **P1**, on PE and PS surfaces demonstrating that favourable serum release can be facilitated by SRPs containing a proportion of biomass-derived monomer **1**. However, the homopolymer **P5** showed no additional benefit compared to the negative control (Nil) highlighting the importance of the aromatic unit in enabling effective modification of PET and PS fabric surfaces.

Taken together, performance studies demonstrate that fabric surface modification has taken place, and show that comparable performance to SRPs currently used in formulations could be achieved on PET fabrics, while incorporating significant quantities of biobased monomer 1. The soil-release and anti-redeposition performance of SRPs containing up to 50% 1 on PET surfaces were also comparable to those reported in our previous study³⁵ which employed biomass-derived pyridine dicarboxylate monomers. In the case of PS, however, the inclusion of monomer 1 improved the performance of SRPs beyond those currently in formulation, offering an enhanced overall environmental profile. The structural factors driving these differences in performance were

Journal Name ARTICLE

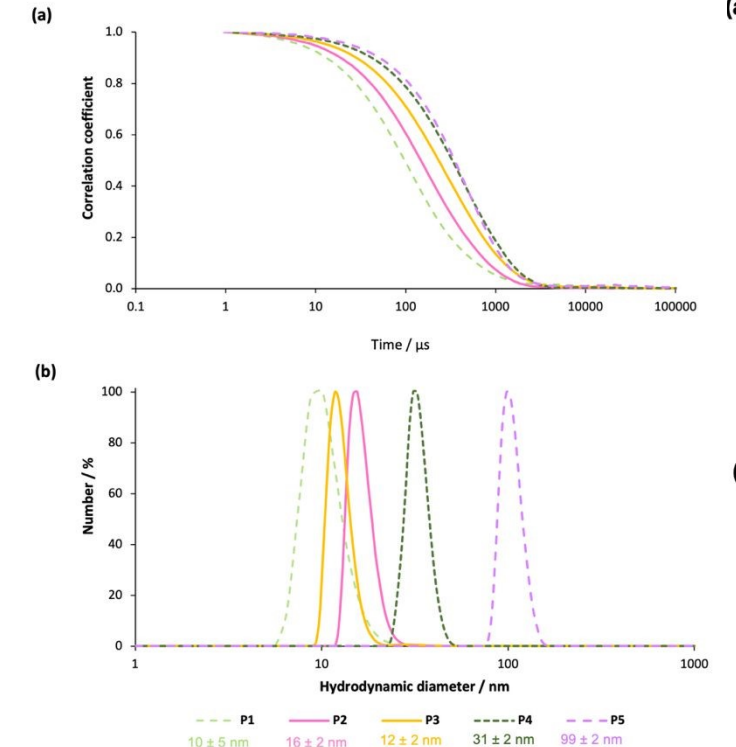


Figure 4: (a) DLS correlation functions. (b) Normalised number average particle size distributions, with indicative average D_h for SRP in an aqueous solution (1.0% w/w), with measurements recorded at 35 °C.

not immediately evident, and we therefore conducted a series of experiments to investigate the solution behaviour and surface activity of SRPs using a simplified representative system.

Solution behaviour of SRPs

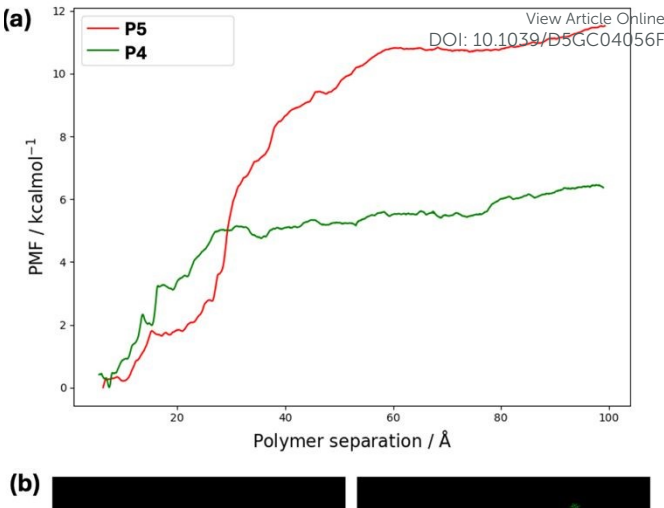
This article is licensed under a Creative Commons Attribution 3.0 Unported Licence.

Open Access Article. Published on 15 octombrie 2025. Downloaded on 17.10.2025 14:13:21

Solutions of P1-P5 in water (1% w/w) were subjected to DLS analysis at 35 °C to investigate the species present in solution (Figure 4). In each case, nanoscale aggregates were observed, with differences in the sizes of the aggregates evident from the correlation functions obtained (Figure 4a).

In line with previous studies,³⁵ we identified a correlation between solution aggregation state and soil release performance. SRPs observed to self-assemble to yield larger aggregates (e.g. **P5** D_h 100 nm at 1% w/w), were found to display poor performance, while polymers observed to form smaller aggregates (e.g. P1-P3 D_h 10-20 nm) were shown to function more effectively.

To understand the factors that contribute to the observed aggregation of DGAX-containing SRPs, umbrella sampling simulations were performed on the association of two molecules of P4, and two molecules of P5, to obtain a potential of mean force (PMF), where the reaction coordinate is the separation between the centre of mass of each core unit (Figure 5a). An aggregate of two polymers was equilibrated in solution using a general molecular dynamics workflow, before steered molecular dynamics (SMD)58 was applied to separate the polymers at a rate of 1 Å ns⁻¹ from the minimum possible distance to a maximum of 99 Å. Snapshots from the SMD simulations were captured at distances from the minimum to



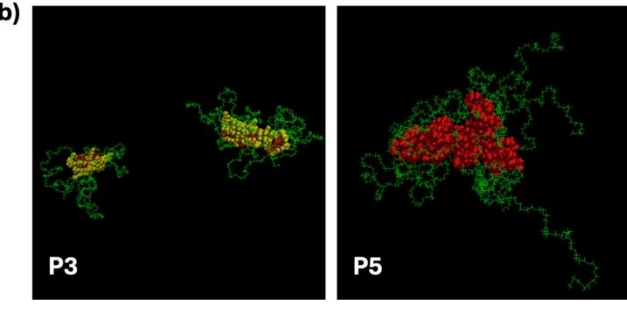


Figure 5: (a) Potential of mean force (PMF) obtained from umbrella sampling calculations for the cores of P5 and P4 as a function of separation between the centres of the polymer chains. (b) Representative snapshots of P3 and P5 at 1% (w/w) solution after 15 ns of simulation time. PEG chains are represented as lines in green, monomer 1 is shown as van der Waals radii in red and monomer 2 is shown as Van der Waals radii in yellow.

99 Å, with a separation of roughly 1 Å between windows. Each window simulation was then run for 40 ns, with a restraint potential of 2.5 kcal mol-1 to keep the polymers in place. The configurations from these simulations were then reweighted using the weighted histogram analysis method (WHAM)59 and combined to generate the PMF for each SRP aggregate complex. The difference in free energy of aggregation can then be derived from the PMF plot by subtracting the energy of the plateau region (full separation) from the energy of the bound state (minimum distance), which is normalised to 0 kcal mol-1.

Simulations suggest that the aggregation of P5 is energetically more favourable than that of P4, with significantly more energy required to separate the cores (Figure 5a). It is likely that this aggregation is driven by strong hydrophobic effects. Affinity between units of 2 is also evidenced in simulations where five P3 and P5 polymer molecules were studied in 1% (w/w) solution (Figure 5b, ESI Section 7.4). Larger aggregates are present after 20 ns for P5 compared to P3, consistent with the observation of larger assemblies in DLS studies. For P3, inter-core interactions are mainly mediated by π - π stacking but this is disrupted by the presence of **1**. Moreover, π - π stacking in water is sufficiently weak to be dynamic^{60, 61}allowing relatively rapid chain refolding, as seen in our previous work on pyridine dicarboxylate-based polymers.³⁵

ARTICLE Journal Name

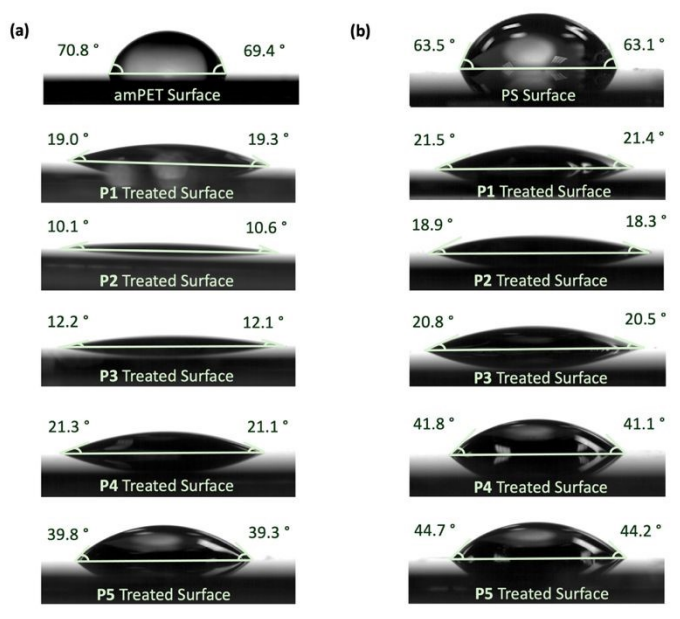


Figure 6: Contact angle measurements of a 5 μ L droplet of deionised water on a (a) amPET surface and 1% (w/w) SRP-treated amPET surface; (b) PS surface and 1% (w/w) SRP-treated PS surface; after dip rinsing in H₂O.

Surface activity of SRPs

A primary function of SRPs is the hydrophilisation of hydrophobic surfaces, proposed to occur through the binding of the hydrophobic block of the polymer to the surface of the fabric, resulting in the hydrophilic blocks being positioned at the aqueous interface through molecular orientation (Figure 1). To investigate the ability of the SRPs to modify fabric surfaces, solutions of P1-P5 were deposited on model surfaces representing the chemical composition of PE and PS fabrics. Model PE surfaces were created by spin-coating a solution of amorphous PET (amPET, 1% w/w in CHCl₄) onto silicon wafer (1500 rpm, 30 s). A similar method was followed to create a surface which approximates the composition of PS, using a blend of amPET and polyurethane (95:5) solution (1% w/w in THF) spin-coated onto a silicon wafer (2000 rpm, 30 s). The model PET and PS surfaces were shown to display average water contact angles of 70.1° and 63.3°, respectively, indicative of hydrophobic surfaces.

Surfaces were then treated with a solution of SRP (**P1-P5**, 1% w/w) for 40 min, then inverted to allow for the removal of undeposited SRP. A 5 μ L droplet of deionised water was then placed on each of the SRP-treated surfaces, with the contact angle measured at room temperature (ESI Figure S4). All surfaces modified with SRP displayed a reduction in the contact angle, ranging from 5.0 ° to 19.4 ° (ESI Figure S4), suggesting deposition of polymer and surface hydrophilisation.

Water contact angles were measured after the SRP-modified surfaces underwent a dip rinse (Figure 6), to better reflect the overall wash process and provide a greater understanding regarding the extent of surface deposition. On PET surfaces treated with **P2-P4**, contact angles between 10.1 and 21.3 ° were observed, in line with the contact angle

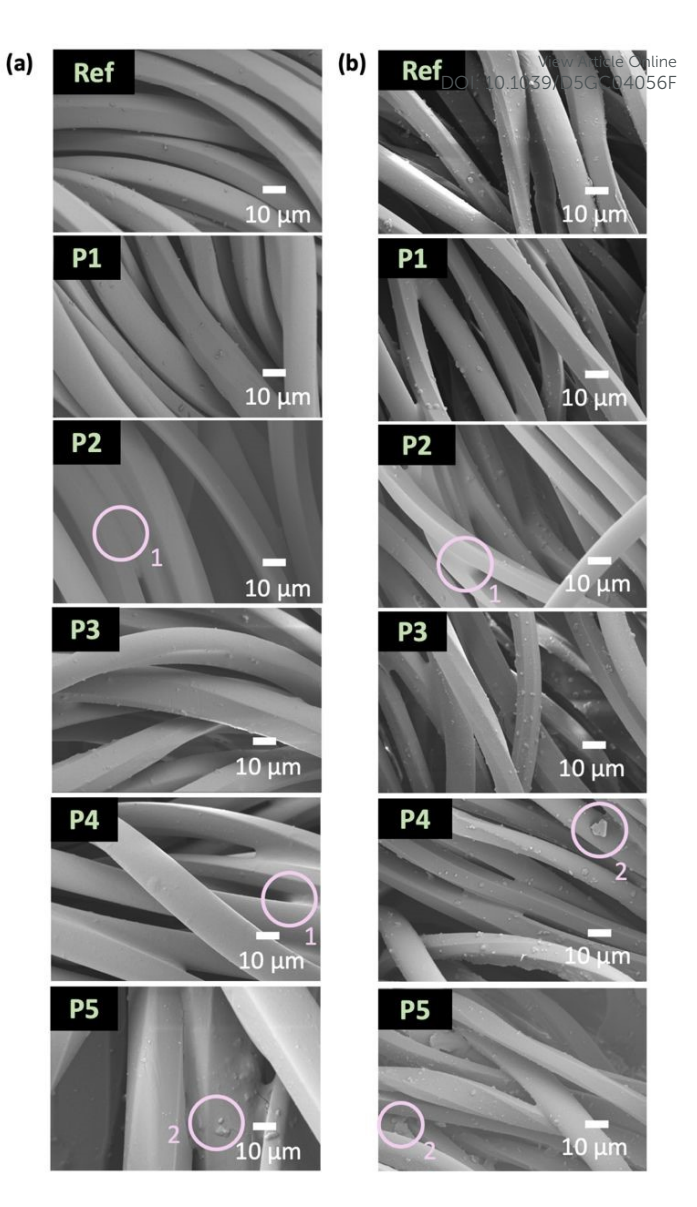


Figure 7: SEM images taken at a magnification of 1,000 × for (a) PET and the PE-SRP modified fabrics (P1 to P5) with a gold-palladium sputter coating thickness of around 33 nm; (b) PS and the PS-SRP modified fabrics (P1 to P5) with a gold-palladium sputter coating thickness of around 49 nm. Some features have been highlighted: 1. SRPs appearing to deposit between fibres; 2. Irregular deposits on fibres.

observed for surfaces treated with **P1** (19.2°), suggesting that surface hydrophilization has been retained. The PET surface treated with **P5** displayed an increased contact angle after rinsing (39.6°), suggesting a decrease in effective SRP surface concentration and increased hydrophobicity, which may account for the poor soil-release performance observed. PS surfaces treated with **P2** and **P3** displayed contact angles after rinsing of 18.3 to 20.5°, in line with that displayed by a surface treated with **P1** and rinsed (21.5°). Surfaces treated with **P4** and **P5** displayed an increased contact angle after rinsing (41.1 - 44.7°). This relative surface hydrophobicity is consistent with the poor performance of these polymers in soil-release tests (Figure 3), suggesting that these SRPs are easily removed from the surface by rinsing.

Journal Name ARTICLE

View Article Online

Table 2: Energies obtained from MM/PBSA calculations for each truncated polymer core on model PET and PS surfaces. The full details of the binding calculations are given in the ESI (Section 7.3), where $\Delta G_{\rm gas} = \Delta G_{\rm complex}$ - $\Delta G_{\rm surface}$ - $\Delta G_{\rm molecule}$ is the binding energy in the absence of any solvent; $\Delta G_{\rm solv}$ is the PBSA solvent corrections to $\Delta G_{
m gas}$; $\Delta G_{
m bind} = \Delta G_{
m gas} + \Delta G_{
m solvent}$; $\Delta G_{
m fold}$ is the folding free energy in implicit solvent; and $\Delta G_{
m bind}' = \Delta G_{
m bind} - \Delta G_{
m fold}$.

Polymer core	Surface	ΔG _{gas} / kcal mol⁻¹	ΔG _{solv} / kcal mol ⁻¹	ΔG _{bind} / kcal mol ⁻¹	ΔG _{fold} / kcal mol⁻¹	ΔG′ _{bind} / kcal mol ⁻¹
P1	PET	-101.63 (0.63)	85.45 (0.40)	-16.18 (0.66)	-9.00 (0.31)	-7.18 (0.73)
P2	PET	-114.98 (0.78)	94.84 (0.51)	-20.14 (0.85)	-10.97 (0.37)	-9.17 (0.93)
Р3	PET	-120.79 (0.84)	99.28 (0.54)	-21.52 (0.89)	-9.37 (0.41)	-12.14 (0.98)
P4	PET	-109.98 (0.77)	89.38 (0.46)	-20.60 (0.79)	-13.51 (0.40)	-7.08 (0.88)
P5	PET	-127.40 (0.87)	100.69 (0.50)	-26.71 (0.90)	-29.29 (0.45)	2.57 (1.01)
P1	PS	-95.16 (0.61)	82.33 (0.40	-12.83 (0.65)	-8.40 (0.30)	-4.43 (0.72)
P2	PS	107.54 (0.77)	90.85 (0.50)	-16.69 (0.84)	-10.44 (0.37)	-6.26 (0.92)
Р3	PS	-115.08 (0.83)	96.32 (0.53)	-18.76 (0.89)	-8.97 (0.41)	-9.79 (0.98)
P4	PS	-105.72 (0.75)	87.53 (0.45)	-18.19 (0.77)	-12.80 (0.39)	-5.39 (0.86)
P5	PS	-122.39 (0.88)	97.89 (0.50)	-24.49 (0.91)	-27.78 (0.45)	3.28 (1.01)

SEM imaging was performed to gain further insight into the deposition of the SRPs on both PET and PS fabric surfaces. Samples for SEM analysis were prepared by soaking $1 \times 1 \text{ cm}^2$ fabric swatches in solutions of P1-P5 (1% w/w) (210 rpm, 35 °C). Fabrics were air dried overnight before sputter coating with a gold-palladium conducting layer. SEM images were then taken at a range of magnifications (Figure 7, ESI Figure S5/S6) to show the morphological changes to fabric fibres as SRP deposit and modify their surface. A reference sample was imaged to allow for a direct comparison between an unmodified and modified fabric surface. In each case, changes in surface morphology were evident, consistent with deposition of SRPs P1-P5 on surfaces.

Image analysis of the reference PET sample (Figure 7a, ESI Figure S5) showed the presence of a textured surface with sharp elements raised on the surface with a maximum length of 2 μ m. Despite these sharp elements remaining present to some extent after SRP-surface modification, surfaces treated with P1-P4 appear smoother, suggesting that SRPs have coated the surface of the fibres. The presence of SRPs was also highlighted by the build-up of polymer in the gaps of the fibres, thereby increasing the surface area and eliminating potential locations for soil to collect (Figure 7a, feature 1). Surfaces treated with poorlyperforming P5 appeared to be more textured, with additional build-up on the surface as the raised elements increased in size to greater than 2 µm and were more irregular in topology compared to the reference fabric. This irregularity in surface topology may partially account for the increased deposition of hydrophobic material on these surfaces.

Images were also collected for PS textiles (Figure 7b, ESI Figure S6). Here, the reference PS showed a highly irregular structure that was very textured with crystalline features. The fabric treated with P1 displayed a similar appearance to the reference fabric, which could contribute to the poor

performance of this SRP. Incubation in solutions of P1-P3 appeared to smooth the surface to varying extents, with notable improvements in morphology noted for P2. Surfaces treated with P4 and P5 displayed similar surface morphologies to unmodified PS, including the presence of irregular deposits Figure 7b, feature 2), which may suggest a higher degree of heterogeneity in surface modification with SRP.

To rationalise the differences in interfacial behaviour observed, we calculated surface binding energies for truncated SRP core units and model PET and PS surfaces using a MM/PBSA⁶² approach (Table 2; ESI Section 7.3). The calculated modified free energy of binding $\Delta G'_{bind}$ represents a combination of energy gained through non-covalent surface association, including van der Waals and electrostatic interactions, solvation effects, and also incorporates the contribution of chain folding in aqueous solution. Notably, the calculated binding energies correlate with the observed performance in anti-redeposition studies (Figure 2b-c). Core structures containing 2, or combinations of 1 and 2, were predicted to interact favourably with both PET and PS surfaces. The addition of 1 to the core was observed to increase affinity to the surfaces (ΔG_{bind}). The overall strongest binding, $\Delta G'_{bind}$, predicted for P3 cores on a PET surface. Calculated $\Delta G'_{bind}$ values for association of copolymer cores P2-P4 with PS surfaces are more favourable than that of P1, explaining their enhanced performance on this substrate. The inclusion of 1 in the core, however, was predicted to increase the favourability of self-association ($\Delta G_{\text{fold}})\text{,}$ in line with PMF calculations demonstrating strong self-interactions (Figure 5a) and the observation of large aggregates in DLS studies (Figure 4b). The surfaces of these large aggregates are likely to be highly hydrophilic as a consequence of the high density of PEG chains within the corona, and they are therefore either unlikely to deposit on a hydrophobic fabric surface, or are likely to be easily

ARTICLE

removed by rinsing. Interestingly, calculations suggested that P5, which contained 1 as the sole dicarboxylate component and displayed poor performance, would interact favourably with PET and PS surfaces (ΔG_{bind}). Effective performance is likely prevented by the tendency of P5 to form large aggregates in solution (Figure 4b), driven by significant self-association (ΔG_{fold}). The inclusion of 2 suppresses aggregation in solution (Figure 4b), with reductions in calculated ΔG_{fold} observed. These observations may suggest that an important role of the terephthalate component in enabling SRP performance within this series is in suppression of aggregation, in addition to directly interacting with the fabric surface, presenting opportunities to replace 2 with another biobased monomer, to further improve the sustainability profile of the SRPs.

Conclusions

This article is licensed under a Creative Commons Attribution 3.0 Unported Licence.

en Access Article. Published on 15 octombrie 2025. Downloaded on 17.10.2025 14:13:21

The incorporation of a proportion of biosourced monomer 1 in SRPs yielded promising performance benefits, matching those of conventional SRP P1 on PET substrates, and exceeding the performance of P1 on PS substrates. While all polymers were demonstrated to modify and hydrophilise representative surfaces through contact angle and SEM studies, we have identified a correlation between solution aggregation and performance which affords molecular-level insight into the mechanism of effective surface modification, and explains differences in performance observed. Polymers which formed smaller aggregates, as assessed through DLS studies, were observed to display enhanced performance in anti-redeposition and soil-release tests compared to those which form larger aggregates. Molecular modelling studies predict this selfassociation behaviour, and suggest that aggregation is driven by strong hydrophobic effects. Binding energies have been calculated for SRPs on model fabric surfaces, calculated using a MM/PBSA method which incorporates surface interaction, solvation and folding effects. These calculations support the differences in performance observed, with polymers predicted to engage in thermodynamically favourable interactions with model surface observed to perform well, while the interaction of polymer P5, which displayed no favourable performance, was predicted to be thermodynamically unfavourable on both PET and PS surfaces. Effective surface modification likely requires binding of individual polymer entities to surfaces, in order for the hydrophobic core to interact with the fabric surface. SRPs that display solution aggregation are likely to display either limited deposition on surfaces, on account of shielding of the hydrophobic core by PEG blocks, or to be readily removed by rinsing.

SRPs containing **1** offer an improved sustainability profile to those currently used in formulation, as their performance extends to PS fabrics, offering the benefits of improved cleaning performance at low wash temperatures to an important class of textiles. A limitation of the SRPs described here is the requirement for the incorporation of terephthalic acid within the central block of the polymer. Developments in the production of biosourced terephthalic acid³¹⁻³³ may offer a route to SRPs with an enhanced sustainability profile.

Alternatively, it is possible that other biosourced monomers, such as the pyridine dicarboxylates used in durprevious study, so or other hemicellulose-derived diacids, could be used to replace the terephthalate component altogether. Furthermore, building on the work of Manker et al, 49 the possibility of preparing polymers directly from hemicellulosic biomass could be explored. SRPs constructed using modified polysaccharides have been demonstrated 13 to display favourable soil-release performance on PET surfaces, highlighting further opportunities in the development of biosourced alternative additives.

Journal Name

In addition to presenting detergent additives of enhanced performance and improved sustainability profile, our studies have additionally enhanced understanding of the mechanism of action of SRPs. This mechanistic understanding will guide in the future design of biosourced SRPs, with a view to improving the environmental footprint of these key additives.

Author contributions

EFF: investigation, methodology, data curation, writing – initial draft; MS: investigation, methodology, data curation; EKF: investigation, methodology, data curation; JB: investigation, methodology, data curation; GS: conceptualisation, resources, supervision, writing – review and editing RC: investigation, methodology, data curation; MRS: resources, writing – review and editing; RLT: resources, supervision, MRW: funding acquisition, investigation, supervision, writing – review and editing; CSM: conceptualisation, funding acquisition, resources, supervision, writing – review and editing.

Conflicts of interest

There are no conflicts to declare.

Data availability

Data supporting this article has been included within the Supporting Information: Synthetic and experimental methods, characterisation, additional performance testing data, calculations.

Acknowledgements

This work was supported by the Engineering and Physical Sciences Research Council [UKRI Future Leaders Fellowship MR/V027018/1; ANTENNA Prosperity Partnership EP/V056891/1; SOFI2 CDT EP/S023631/1].

Notes and references

1. Rodriquez F., Cohen C., Ober C. K. and Archer L. A., *Principles of Polymer Systems*, CRC Press, Boca Raton Florida, Sixth edn., 2015.

ARTICLE Journal Name

- 2. Zhang Z., Huang J., Yao Y., Peters G., Macdonald B., La Rosa A. D., Wang Z. and Scherer L., Nat. Rev. Earth Environ., 2023, 4, 703-715.
- 3. Fixing fashion: clothing consumption and sustainability, Environmental Audit Committee, House of Commons,
- 4. Valuing our clothes: The cost of UK fashion, WRAP, 2017.
- 5. Preferred Fiber & Materials Market Report, Textile Exchange, 2021.
- 6. Chen S., Zhang S., Galluzzi M., Li F., Zhang X., Yang X., Liu X., Cai X., Zhu X., Du B., Li J. and Huang P., Chem. Eng. J., 2019, **358**, 634–642.
- 7. Chi Y.-S. and Obendorf S. K., J. Surfactants Deterg., 1999, 2,
- 8. Cooper T. and Claxton S., J. Clean. Prod., 2022, 351, 131394.
- 9. Herreweghen F. V., Amberg C., Marques R. and Callewaert C., Microorganisms, 2020, 8, 1709.
- 10. Abdul-Bari M. M., McQueen R. H., de la Mata A. P., Batchellet J. C. and Harynuk J. J., Text. Res. J., 2020, 90, 2212-2222.
- 11. Kan C. W. and Yuen C. W. M., Nucl. Instrum. Methods Phys. Res. B., 2008, 266, 127-132.
- 12. F. W. Marco and P. G. Harris, EP. Pat., EP0023361B1, 1983.
- 13. D'Avino M., Chilton R., Si G., Sivik M. R. and Fulton D. A., Ind. Eng. Chem. Res., 2022, 61, 14159-14172.
- 14. R. P. Rudy and A. A. Romano, US Pat., US 6426379B1, 2002.
- 15. Boardman S. J., Hayward A. S., Lant N. J., Fossum R. D. and Thornton P. D., J. Appl. Polym. Sci., 2021, 138, 49632.
- 16. V. N. G. Kumar and A. Moulee, US. Pat., US 6764992B2, 2004.
- 17. Rathinamoorthya R., Ayswarriya N., Kadambari R., Sreelatha R. and Janani K. G., Indian J. Fibre Text. Res., 2016, 41, 432-439.
- Save Energy in Your Home, Energy Saving Trust 2017. 18.
- Pavlidou S. and Paul R., 3 Moisture management and soil release finishes for textiles, Woodhead, Woodhead Publishing Series in Textiles, 2015.
- 20. Valentini A., Bakalis S., Gkatzionis K., Palazzo G., Cioffi N., Di Franco C., Robles E., Brooker A. and Britton M. M., Ind. Eng. Chem. Res., 2019, 58, 14839-14847.
- P. Barreleiro, M. Weide, M. Hutmacher, R. Simmering and 21. N. Wrubbel, WO. Pat., WO2014079755, 2015.
- P.-P. Vinuesa, E. Maria and M. Jennewein, EP. Pat., 22. EP2135931, 2009.
- 23. M. Peeters, A. Jacques and D. More, WO. Pat., WO2007059532, 2006.
- S. D. Melvin Carvell, Kenneth Metcalfe, John William Harold Yorke, EP Pat., EP3650522, 2018.
- 25. G. Si, M. McDonnell, M. Gillissen and H. Yamada, WO. Pat., WO2021118814, 2021.
- M. Gillissen, H. Yamada, G. Si and M. McDonnell, WO. Pat., 26. WO2021116049, 2019.
- 27. K. L. M. Depoot and J. A. A. Maes, EP. Pat., EP3587546,
- R. Langevin, R. Panandiker and B. Loughnane, WO. Pat., 28. WO2020005879A1, 2018.
- A. Guttentag, WO. Pat., WO2022072399, 2022. 29.
- Tomás R. A. F., Bordado J. C. M. and Gomes J. F. P., Chem. 30. Rev., 2013, 113, 7421-7469.
- 31. M. Volanti, D. Cespi, F. Passarini, E. Neri, F. Cavani, P. Mizsey and D. Fozer, Green Chem., 2019, 21, 885-896.

- Y. Tachibana, S. Kimura and K.-i. Kasuya, Sci. Rep 2015, 5. DOI: 10.1039/D5GC04056F
- 33. J. Louw, S. Farzad and J. F. Görgens, Biochem. Eng. J., 2024, **210**, 109404.
- UKBioChem10: The Ten Green Chemicals which can Create 34. Growth, Jobs and Trade for the UK, The Lignocellulosic Biorefinery Network, 2019.
- 35. M. Starck, E. F. Fiandra, J. Binks, G. Si, R. Chilton, M. Sivik, R. L. Thompson, J. Li, M. R. Wilson and C. S. Mahon, JACS Au, 2025, 5, 666-674.
- 36. Fiandra E. F., Shaw L., Starck M., McGurk C. J. and Mahon C. S., Chem. Soc. Rev., 2023, 52, 8085-8105.
- Sousa A. F., Vilela C., Fonseca A. C., Matos M., Freire C. S. R., Gruter G. J. M., Coelho J. F. J. and Silvestre A. J. D., Polym. Chem., 2015, 6, 5961-5983.
- 38. Delidovich I., Hausoul P. J. C., Deng L., Pfützenreuter R., Rose M. and Palkovits R., Chem. Rev., 2016, 116, 1540-1599.
- Pellis A., Comerford J. W., Weinberger S., Guebitz G. M., 39. Clark J. H. and Farmer T. J., Nat. Commun., 2019, 10, 1762.
- 40. O'Dea R. M., Willie J. A. and Epps III T. H., ACS Macro. Lett., 2020, 9, 476-493.
- 41. Isikgor F. H. and Becer C. R., Polym. Chem., 2015, 6, 4497-
- 42. Huber G. W., Iborra S. and Corma A., Chem. Rev., 2006, **106**, 4044-4098.
- 43. Deng W., Feng Y., Fu J., Guo H., Guo Y., Han B., Jiang Z., Kong L., Li C., Liu H., Nguyen P. T. T., Ren P., Wang F., Wang S., Wang Y., Wang Y., Wong S. S., Yan K., Yan N., Yang X., Zhang Y., Zhang Z., Zeng X. and Zhou H., Green Energy Environ., 2023, 8, 10-114.
- Houfani A. A., Anders N., Spiess A. C., Baldrian P. and 44. Benallaoua S., Biomass Bioenergy, 2020, 134, 105481.
- 45. Scheller H. V. and Ulvskov P., Annu. Rev. Plant Biol., 2010,
- Huang L.-Z., Ma M.-G., Ji X.-X., Choi S.-E. and Si C., Front. 46. Bioeng. Biotechnol., 2021, 9, 690773.
- 47. Gabov K., Gosselink R. J. A., Smeds A. I. and Fardim P., J. Agric. Food Chem., 2014, 62, 10759-10767.
- 48. Gandam P. K., Chinta M. L., Pabbathi N. P. P., Velidandi A., Sharma M., Kuhad R. C., Tabatabaei M., Aghbashlo M., Baadhe R. R. and Gupta V. K., J. Energy Inst., 2022, 101, 290-308.
- Manker L. P., Dick G. R., Demongeot A., Hedou M. A., 49. Rayroud C., Rambert T., Jones M. J., Sulaeva I., Vieli M., Leterrier Y., Potthast A., Maréchal F., Michaud V., Klok H.-A. and Luterbacher J. S., Nat. Chem., 2022, 14, 976–984.
- 50. S. Zheng, S. Sun, L. P. Manker and J. S. Luterbacher, Acc. Chem. Res., 2025, 58, 877-892.
- 51. S. Bertella, A. Komarova, S. Sun and J. Luterbacher, EP. Pat., EP4311826, 2022.
- A. Komarova, S. Sun, S. Bertella and J. Luterbacher, WO. 52. Pat., WO2023198682, 2023.
- 53. S. Bertella, A. Komarova, S. Sun and J. Luterbacher, EP. Pat., EP4311831 2022.
- J. Ruwoldt, F. H. Blindheim and G. Chinga-Carrasco, RSC 54. Adv., 2023, 13, 12529-12553.
- 55. Matyjaszewski K. and Möller M., Polymer Science: A Comprehensive Reference Volume 5: Polycondensation, Elsevier, 2013.
- 56. A. Ketema and A. Worku, J. Chem., 2020, 2020, 6628404.
- 57. Colorimetry, ISO/CIE 11664-4:2019(E), 1976.

ARTICLE

Journal Name

Green Chemistry Accepted Manuscript

View Article Online DOI: 10.1039/D5GC04056F

58. H. Grubmüller, B. Heymann and P. Tavan, *Science*, 1996, **271**, 997–999.

- S. Kumar, J. M. Rosenberg, D. Bouzida, R. H. Swendsen and P. A. Kollman, *J. Comp. Chem.*, 1992, 13, 1011–1021.
- F. Chami and M. R. Wilson, J. Am. Chem. Soc., 2010, 132, 7794–7802.
- G. Yu, M. Walker and M. R. Wilson, *Phys. Chem. Chem. Phys.*, 2021, 23, 6408–6421.
- E. Wang, H. Sun, J. Wang, Z. Wang, H. Liu, J. Z. H. Zhang and T. Hou, *Chem. Rev.*, 2019, **119**, 9478–9508.

View Article Online DOI: 10.1039/D5GC04056F

Data availability

Data supporting this article has been included within the Supporting Information: Synthetic methods, experimental methods, characterisation data, calculations.